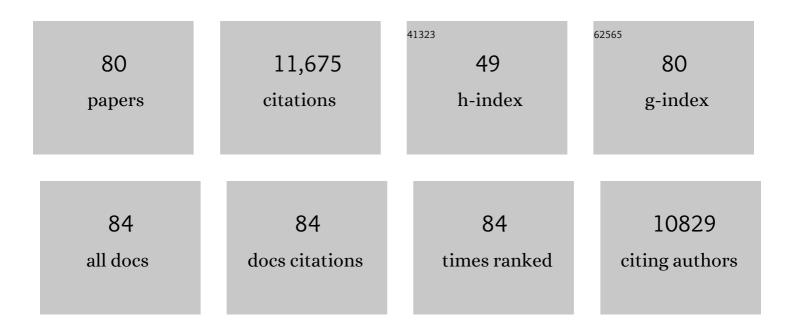
Qinghong Zhang

List of Publications by Year in descending order

Source: https://exaly.com/author-pdf/767469/publications.pdf Version: 2024-02-01



#	Article	IF	CITATIONS
1	Electrocatalytic reduction of CO2 to ethylene and ethanol through hydrogen-assisted C–C coupling over fluorine-modified copper. Nature Catalysis, 2020, 3, 478-487.	16.1	788
2	New horizon in C1 chemistry: breaking the selectivity limitation in transformation of syngas and hydrogenation of CO ₂ into hydrocarbon chemicals and fuels. Chemical Society Reviews, 2019, 48, 3193-3228.	18.7	742
3	Development of Novel Catalysts for Fischer–Tropsch Synthesis: Tuning the Product Selectivity. ChemCatChem, 2010, 2, 1030-1058.	1.8	665
4	Nanocomposites of TiO ₂ and Reduced Graphene Oxide as Efficient Photocatalysts for Hydrogen Evolution. Journal of Physical Chemistry C, 2011, 115, 10694-10701.	1.5	582
5	Photocatalytic and photoelectrocatalytic reduction of CO ₂ using heterogeneous catalysts with controlled nanostructures. Chemical Communications, 2016, 52, 35-59.	2.2	508
6	Direct and Highly Selective Conversion of Synthesis Gas into Lower Olefins: Design of a Bifunctional Catalyst Combining Methanol Synthesis and Carbon–Carbon Coupling. Angewandte Chemie - International Edition, 2016, 55, 4725-4728.	7.2	468
7	Promoting electrocatalytic CO2 reduction to formate via sulfur-boosting water activation on indium surfaces. Nature Communications, 2019, 10, 892.	5.8	446
8	Solar energy-driven lignin-first approach to full utilization of lignocellulosic biomass under mild conditions. Nature Catalysis, 2018, 1, 772-780.	16.1	442
9	Photocatalytic transformations of lignocellulosic biomass into chemicals. Chemical Society Reviews, 2020, 49, 6198-6223.	18.7	374
10	Base-Free Aerobic Oxidation of 5-Hydroxymethyl-furfural to 2,5-Furandicarboxylic Acid in Water Catalyzed by Functionalized Carbon Nanotube-Supported Au–Pd Alloy Nanoparticles. ACS Catalysis, 2014, 4, 2175-2185.	5.5	353
11	Sulfur vacancy-rich MoS2 as a catalyst for the hydrogenation of CO2 to methanol. Nature Catalysis, 2021, 4, 242-250.	16.1	308
12	Conversion of Cellulose into Sorbitol over Carbon Nanotube-Supported Ruthenium Catalyst. Catalysis Letters, 2009, 133, 167-174.	1.4	290
13	Zeoliteâ€Encaged Singleâ€Atom Rhodium Catalysts: Highlyâ€Efficient Hydrogen Generation and Shapeâ€Selective Tandem Hydrogenation of Nitroarenes. Angewandte Chemie - International Edition, 2019, 58, 18570-18576.	7.2	281
14	Electrocatalytic reduction of CO ₂ and CO to multi-carbon compounds over Cu-based catalysts. Chemical Society Reviews, 2021, 50, 12897-12914.	18.7	266
15	Selective transformation of carbon dioxide into lower olefins with a bifunctional catalyst composed of ZnGa ₂ 0 ₄ and SAPO-34. Chemical Communications, 2018, 54, 140-143.	2.2	265
16	CdS–graphene and CdS–CNT nanocomposites as visible-light photocatalysts for hydrogen evolution and organic dye degradation. Catalysis Science and Technology, 2012, 2, 969.	2.1	261
17	Subnanometer Bimetallic Platinum–Zinc Clusters in Zeolites for Propane Dehydrogenation. Angewandte Chemie - International Edition, 2020, 59, 19450-19459.	7.2	221
18	Oxidative conversion of lignin and lignin model compounds catalyzed by CeO ₂ -supported Pd nanoparticles. Green Chemistry, 2015, 17, 5009-5018.	4.6	210

QINGHONG ZHANG

#	Article	IF	CITATIONS
19	Design of efficient bifunctional catalysts for direct conversion of syngas into lower olefins <i>via</i> methanol/dimethyl ether intermediates. Chemical Science, 2018, 9, 4708-4718.	3.7	208
20	TiO ₂ -based heterojunction photocatalysts for photocatalytic reduction of CO ₂ into solar fuels. Journal of Materials Chemistry A, 2018, 6, 22411-22436.	5.2	195
21	Visible light-driven Câ^H activation and C–C coupling of methanol into ethylene glycol. Nature Communications, 2018, 9, 1181.	5.8	188
22	Sizeâ€Dependent Catalytic Activity of Supported Palladium Nanoparticles for Aerobic Oxidation of Alcohols. Advanced Synthesis and Catalysis, 2008, 350, 453-464.	2.1	174
23	Fischer–Tropsch Catalysts for the Production of Hydrocarbon Fuels with High Selectivity. ChemSusChem, 2014, 7, 1251-1264.	3.6	164
24	Tandem Catalysis for Hydrogenation of CO and CO ₂ to Lower Olefins with Bifunctional Catalysts Composed of Spinel Oxide and SAPO-34. ACS Catalysis, 2020, 10, 8303-8314.	5.5	157
25	Single-pass transformation of syngas into ethanol with high selectivity by triple tandem catalysis. Nature Communications, 2020, 11, 827.	5.8	156
26	Direct Conversion of Syngas into Methyl Acetate, Ethanol, and Ethylene by Relay Catalysis via the Intermediate Dimethyl Ether. Angewandte Chemie - International Edition, 2018, 57, 12012-12016.	7.2	142
27	Recent advances in understanding the key catalyst factors for Fischer-Tropsch synthesis. Journal of Energy Chemistry, 2013, 22, 27-38.	7.1	130
28	Ligand-Controlled Photocatalysis of CdS Quantum Dots for Lignin Valorization under Visible Light. ACS Catalysis, 2019, 9, 8443-8451.	5.5	128
29	Hydrous ruthenium oxide supported on Co3O4 as efficient catalyst for aerobic oxidation of amines. Green Chemistry, 2008, 10, 553.	4.6	111
30	Catalytic Conversion of Ethylene to Propylene and Butenes over Hâ^'ZSM-5. Industrial & Engineering Chemistry Research, 2009, 48, 10788-10795.	1.8	111
31	Photocatalytic and electrocatalytic transformations of C1 molecules involving C–C coupling. Energy and Environmental Science, 2021, 14, 37-89.	15.6	110
32	Transformation of cellulose and related carbohydrates into lactic acid with bifunctional Al(<scp>iii</scp>)–Sn(<scp>ii</scp>) catalysts. Green Chemistry, 2018, 20, 735-744.	4.6	109
33	Metal Sulfide Photocatalysts for Lignocellulose Valorization. Advanced Materials, 2021, 33, e2007129.	11.1	106
34	Visualizing Element Migration over Bifunctional Metalâ€Zeolite Catalysts and its Impact on Catalysis. Angewandte Chemie - International Edition, 2021, 60, 17735-17743.	7.2	99
35	Effect of size of catalytically active phases in the dehydrogenation of alcohols and the challenging selective oxidation of hydrocarbons. Chemical Communications, 2011, 47, 9275.	2.2	96
36	Oxidative Dehydrogenation of Propane to Propylene in the Presence of HCl Catalyzed by CeO ₂ and NiO-Modified CeO ₂ Nanocrystals. ACS Catalysis, 2018, 8, 4902-4916.	5.5	95

QINGHONG ZHANG

#	Article	IF	CITATIONS
37	Osmium-Catalyzed Selective Oxidations of Methane and Ethane with Hydrogen Peroxide in Aqueous Medium. Advanced Synthesis and Catalysis, 2007, 349, 1199-1209.	2.1	94
38	Visibleâ€Lightâ€Driven Cleavage of Câ^'O Linkage for Lignin Valorization to Functionalized Aromatics. ChemSusChem, 2019, 12, 5023-5031.	3.6	86
39	Monodispersed sub-5.0 nm PtCu nanoalloys as enhanced bifunctional electrocatalysts for oxygen reduction reaction and ethanol oxidation reaction. Nanoscale, 2017, 9, 2963-2968.	2.8	85
40	Solvent-Free Aerobic Oxidation of Alcohols Catalyzed by an Efficient and Recyclable Palladium Heterogeneous Catalyst. Advanced Synthesis and Catalysis, 2005, 347, 1356-1360.	2.1	84
41	Catalytic transformations of cellulose and its derived carbohydrates into 5-hydroxymethylfurfural, levulinic acid, and lactic acid. Science China Chemistry, 2015, 58, 29-46.	4.2	76
42	Hydrogenation of carbon dioxide to light olefins over non-supported iron catalyst. Chinese Journal of Catalysis, 2013, 34, 956-963.	6.9	71
43	Catalytic Transformation of Cellulose and Its Derivatives into Functionalized Organic Acids. ChemSusChem, 2018, 11, 1995-2028.	3.6	71
44	C–H activations of methanol and ethanol and C–C couplings into diols by zinc–indium–sulfide under visible light. Chemical Communications, 2020, 56, 1776-1779.	2.2	59
45	Cobalt and Copper Composite Oxides as Efficient Catalysts for Preferential Oxidation of CO in H2-Rich Stream. Catalysis Letters, 2009, 127, 377-385.	1.4	58
46	Preparation, Characterization and Catalytic Activity of Palladium Nanoparticles Encapsulated in SBA-15. Catalysis Letters, 2008, 120, 126-136.	1.4	54
47	Impact of hierarchical pore structure on the catalytic performances of MFI zeolites modified by ZnO for the conversion of methanol to aromatics. Catalysis Science and Technology, 2017, 7, 3598-3612.	2.1	54
48	Efficient Catalysts for the Green Synthesis of Adipic Acid from Biomass. Angewandte Chemie - International Edition, 2021, 60, 4712-4719.	7.2	54
49	Visualizing Element Migration over Bifunctional Metalâ€Zeolite Catalysts and its Impact on Catalysis. Angewandte Chemie, 2021, 133, 17876-17884.	1.6	53
50	Niobic Acid Nanosheets Synthesized by a Simple Hydrothermal Method as Efficient BrÃ,nsted Acid Catalysts. Chemistry of Materials, 2013, 25, 3277-3287.	3.2	50
51	Selective Conversion of Syngas to Aromatics over a Moâ^'ZrO ₂ /Hâ€ZSMâ€5 Bifunctional Catalyst. ChemCatChem, 2019, 11, 1681-1688.	1.8	50
52	Subnanometer Bimetallic Platinum–Zinc Clusters in Zeolites for Propane Dehydrogenation. Angewandte Chemie, 2020, 132, 19618-19627.	1.6	47
53	Zirconia-supported rhenium oxide as an efficient catalyst for the synthesis of biomass-based adipic acid ester. Chemical Communications, 2019, 55, 11017-11020.	2.2	40
54	Ru particle size effect in Ru/CNT-catalyzed Fischer-Tropsch synthesis. Journal of Energy Chemistry, 2013, 22, 321-328.	7.1	39

QINCHONG ZHANG

#	Article	IF	CITATIONS
55	Superior catalytic performance of phosphorus-modified molybdenum oxide clusters encapsulated inside SBA-15 in the partial oxidation of methane. New Journal of Chemistry, 2003, 27, 1301.	1.4	37
56	Development of Bifunctional Catalysts for the Conversions of Cellulose or Cellobiose into Polyols and Organic Acids in Water. Catalysis Surveys From Asia, 2012, 16, 91-105.	1.0	36
57	Photoelectrocatalytic reduction of CO ₂ to syngas over Ag nanoparticle modified p-Si nanowire arrays. Nanoscale, 2019, 11, 12530-12536.	2.8	36
58	NiO–polyoxometalate nanocomposites as efficient catalysts for the oxidative dehydrogenation of propane and isobutane. Chemical Communications, 2009, , 2376.	2.2	31
59	Selective Hydrogenation of CO ₂ to Ethanol over Sodium-Modified Rhodium Nanoparticles Embedded in Zeolite Silicalite-1. Journal of Physical Chemistry C, 2021, 125, 24429-24439.	1.5	31
60	Distance for Communication between Metal and Acid Sites for Syngas Conversion. ACS Catalysis, 2022, 12, 8793-8801.	5.5	31
61	Photocatalytic coupling of formaldehyde to ethylene glycol and glycolaldehyde over bismuth vanadate with controllable facets and cocatalysts. Catalysis Science and Technology, 2017, 7, 923-933.	2.1	30
62	Direct conversion of syngas into aromatics over a bifunctional catalyst: inhibiting net CO ₂ release. Chemical Communications, 2020, 56, 5239-5242.	2.2	30
63	Z-Scheme nanocomposite with high redox ability for efficient cleavage of lignin C–C bonds under simulated solar light. Green Chemistry, 2021, 23, 10071-10078.	4.6	30
64	Functionalized Carbon Materials in Syngas Conversion. Small, 2021, 17, e2007527.	5.2	29
65	Upcycling Plastic Wastes into Valueâ€Added Products by Heterogeneous Catalysis. ChemSusChem, 2022, 15, .	3.6	29
66	Zeoliteâ€Encaged Singleâ€Atom Rhodium Catalysts: Highlyâ€Efficient Hydrogen Generation and Shapeâ€Selective Tandem Hydrogenation of Nitroarenes. Angewandte Chemie, 2019, 131, 18743-18749.	1.6	26
67	Finely Composition-Tunable Synthesis of Ultrafine Wavy PtRu Nanowires as Effective Electrochemical Sensors for Dopamine Detection. Langmuir, 2017, 33, 8070-8075.	1.6	25
68	Direct conversion of formaldehyde to ethylene glycol via photocatalytic carbon–carbon coupling over bismuth vanadate. Catalysis Science and Technology, 2016, 6, 6485-6489.	2.1	20
69	Catalytic selective oxidation or oxidative functionalization of methane and ethane to organic oxygenates. Science China Chemistry, 2010, 53, 337-350.	4.2	18
70	Lithium ion-exchanged zeolite faujasite as support of iron catalyst for Fischer-Tropsch synthesis. Catalysis Letters, 2007, 114, 178-184.	1.4	15
71	Reaction coupling as a promising methodology for selective conversion of syngas into hydrocarbons beyond Fischer-Tropsch synthesis. Science China Chemistry, 2017, 60, 1382-1385.	4.2	15
72	Cs-substituted tungstophosphate-supported ruthenium nanoparticles as efficient and robust bifunctional catalysts for the conversion of inulin and cellulose into hexitols in water in the presence of H ₂ . RSC Advances, 2014, 4, 43131-43141.	1.7	12

QINGHONG ZHANG

#	Article	IF	CITATIONS
73	Investigation of the Electronic Structure of CdS Nanoparticles with Sum Frequency Generation and Photoluminescence Spectroscopy. Journal of Physical Chemistry C, 2019, 123, 27712-27716.	1.5	12
74	Catalytic conversion of methyl chloride to lower olefins over modified H-ZSM-34. Chinese Journal of Catalysis, 2013, 34, 2047-2056.	6.9	10
75	Selective Transformation of Methanol to Ethanol in the Presence of Syngas over Composite Catalysts. ACS Catalysis, 2022, 12, 8451-8461.	5.5	9
76	Copper–cobalt catalysts supported on mechanically mixed HZSM-5 and γ-Al2O3 for higher alcohols synthesis via carbon monoxide hydrogenation. RSC Advances, 2019, 9, 14592-14598.	1.7	7
77	Functionalized Carbon Materials in Syngas Conversion (Small 48/2021). Small, 2021, 17, 2170256.	5.2	6
78	Frontispiece: Subnanometer Bimetallic Platinum–Zinc Clusters in Zeolites for Propane Dehydrogenation. Angewandte Chemie - International Edition, 2020, 59, .	7.2	5
79	Innentitelbild: Zeoliteâ€Encaged Singleâ€Atom Rhodium Catalysts: Highlyâ€Efficient Hydrogen Generation and Shapeâ€Selective Tandem Hydrogenation of Nitroarenes (Angew. Chem. 51/2019). Angewandte Chemie, 2019, 131, 18466-18466.	1.6	0
80	Frontispiz: Subnanometer Bimetallic Platinum–Zinc Clusters in Zeolites for Propane Dehydrogenation. Angewandte Chemie, 2020, 132, .	1.6	0